



Gap-Filling Restoration Methods for ETM₊ Sensor Images

S.M. Ali* , M.J. Mohammed

Remote Sensing Unit, College of Science, University of Baghdad ,Baghdad, Iraq.

*sensing.remote@gmail.com

Abstract

Enhanced Thematic Mapper Plus (ETM₊) onboard the Landsat-7 remotely sensor satellite was launched on 15 April 1999. On May 31, 2003, image acquisition via the ETM₊ was greatly impacted by the failure of the system's Scan Line Corrector (SLC). Consequently, the ETM₊ has lost approximately 22% of the data due to the increased scan gap. In this work, several gap-filling methods will be proposed to restore the ETM₊ image malfunctions. Some of the proposed methods will be carried by estimating the missed pixel's values from the same image pixel's neighborhood, while others will utilize the pixel values extracted from different temporal scene acquired in different time. Mean average filter, median filter, midpoint filter, and several interpolations (e.g. 1D-nearest neighbor, 1D-linear, and 1D-cubic-spline interpolations) techniques will be utilized to estimate the missed pixel's values from the same malfunction scene and from different temporally radiance corrected scene. Additionally, the Linear Local Histogram Matching (LLHM) technique will be implemented to fill the gaps by gain-bias method and by gray-level normalization methods, using the whole image values first, and a window's values second.

Keywords: ETM₊Malfunction Restoration Methods, Gap-Filling Methods, Interpolation Method.

طرق ترميم لملى ثغرات صور المتحسس ETM₊

صالح مهدي علي* , محمد جمال محمد

وحدة الاستشعار عن بعد، كلية العلوم، جامعة بغداد، بغداد، العراق

الخلاصة

تم إطلاق المتحسس ETM₊ بواسطة التابع لاندسات-7 في 15 نيسان عام 1999، في 31 حزيران عام 2003 تأثر النظام-الماسح-الخطي-المصحح أخفاً كبيراً نتج عنه فقدان ما يقارب 22% من البيانات في المشهد الواحد. في بحثنا الحالي، تم اقتراح العديد من الطرق لترميم القصور في الصور بتعبيثها، بعض الطرق المقترحة تعتمد مبدأ تخمين القيم المفقودة لنقاط الصورة من مجاوراتها، بينما تستخدم الطرق الأخرى قيم نقاط صور ملتقطة بأزمنة مختلفة. لذا سوف نستخدم طرق متعددة لتخمين قيم الثغرات من مشهد الصورة ذاتها والتي تعاني قصوراً وهي مرشح الوسيط المعدل، مرشح المتوسط، مرشح النقطة الوسطى إضافة للعديد من تقنيات الاستكمال (مثل طريقة استكمال المجاور الأقرب، طريقة الاستكمال الخطي، وطريقة الاستكمال التكميلي). كما سوف نستخدم تقنيات أخرى لردم الثغرات من مشاهد ثانية منها تقنية موائمة المخطط التكراري الموضوعي خطياً والذي يعتمد مبدأ معايرة قيم الشدة في الصور باستخدام طريقة الريح-الانحيازي باعتماد قيم شدة الصورة جميعاً أولاً وقيم نافذة من الصورة ثانياً.

1. Introduction

Historically, the meteorological satellite data (low spatial resolution $\approx 1\text{km}$) have been available since the 1960s, while the civilian remote sensing of the Earth's surface from space (medium spatial resolutions $\approx 250\text{ m}$) only began in 1972 with the launch of the first of a series of Earth Resource Satellites; i.e. Landsat. Therefore, the launch of the first civilian remote sensing satellite can be dated as the beginning of significant research activity in remote sensing technology, data analysis and applications, which continue today. In fact, the last 10 years have witnessed a propagation of satellite platforms with higher spatial-resolution "SR" sensors; e.g. SPOT (SR $\approx 20\text{-}5\text{m}$), IKONOS (SR $\approx 4\text{-}1\text{m}$), and QuickBird (SR $\approx 3.2\text{-}0.82\text{m}$). The intensifying of the number of satellite platforms has acquired thousands of trillions of bytes of data invaluable for planning and land management applications [1].

The TM and ETM+ sensors (SR $\approx 30\text{m}$) on board Landsats 5 to 7 have been the most valuable tools over the past three decades for many investigators. The spatial and spectral characteristics of these sensors offered valuable data sets to the community of remote sensing and environmental scientists and final users of remote sensing imagery till the malfunctioning of the SLC on May 31, 2003 which interrupted this valuable source of space-borne imagery [2]. The ETM+ was greatly impacted by the failure of the system's SLC [3], and has lost approximately 22% of the data due to the increased scan gap.

Gapping is a typical phenomenon with remote sensing imagery, it could have dynamic and diverse characteristics thus there are a variety of techniques that could be applied to recover it. Removing gapped areas from satellite imagery is of high interest for visual image interpretation and digital image classification purposes. Imagery gaps could be produced by several reasons; e.g. cloud coverage for optical imagery, shadowed area for SAR data sets, or instrumentation errors (e.g. SLC-off problem) [3], The gap filling is the heart of our present research.

2. Sample of ETM+ Images Experienced SLC Malfunction

The chosen sample of ETM+ multispectral image is located approximately 70 km west of **Kirkuk province, Hawijah City in the North**

of Iraq. The image enclosed area $\approx 943\text{km}$, having the geographic coordinates Lat ($35^{\circ}9'45.34''$ to $35^{\circ}26'7.77''$)N, and Lon ($43^{\circ}29'2.04''$ to $43^{\circ}49'2.02''$)E. It has been acquired on May 14th, 2010, size 1024×1024 pixels, dominated by dry agricultural land, mountain bed rocks and bare soils, and sedimentary materials. Only three bands of these multispectral images have been chosen, shown in Figure 1, to evaluate, objectively and subjectively, the performance of the gap-filling methods. The true color mixing version of the three bands (as RGB) is illustrated in Figure 2.

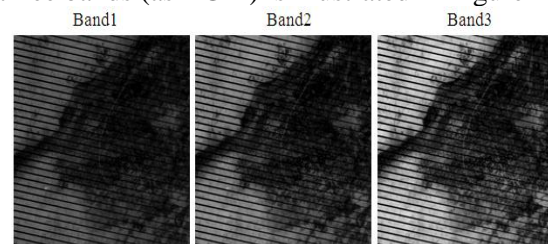


Figure 1-The malfunction multispectral ETM+ bands, acquired in May 14th, 2010



Figure 2- The RGB color scene for the bands shown in Figure 1

The second set is acquired on June 16th, 2010 shown Figure 3, their color version is in Figure 4. They will be used to correct the malfunction scene by interpolating their unaffected pixels in the processed bands gaps.

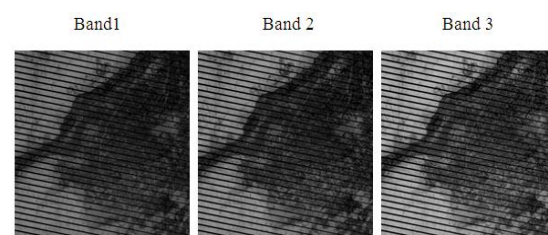


Figure 3- The Multispectral bands of the same scene acquired in June 16th, 2010

3. Gap-Filling (Interpolation) Methodologies

Interpolation is the process used to estimate an image value at a location in between image pixels. For example, in image resizing process in which the output image contains more pixels than it did originally, the interpolation is used to determine the values for the additional interpolate pixels. In our present work, the interpolation will be used to fill the gaps in the malfunction bands of ETM+ image. The gap's values will be estimated by two methods; first the estimation will be carried on the same malfunction image band, second the gap's filling will be from the temporally different scene, where the missed recorded pixels are positioned in different locations. The adopted filling methods will be discussed in the following;

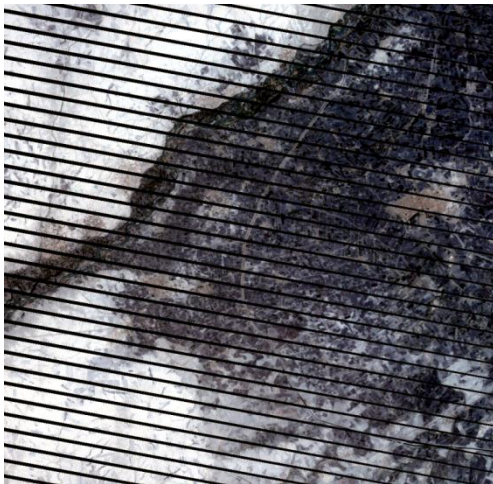


Figure 4- The colored version scene of the agebands shown in Figure 3

For the purpose of quantification, unaffected image bands acquired in January 23rd 2003 has been chosen, shown in Figure 5, to compare the corrected bands with them.

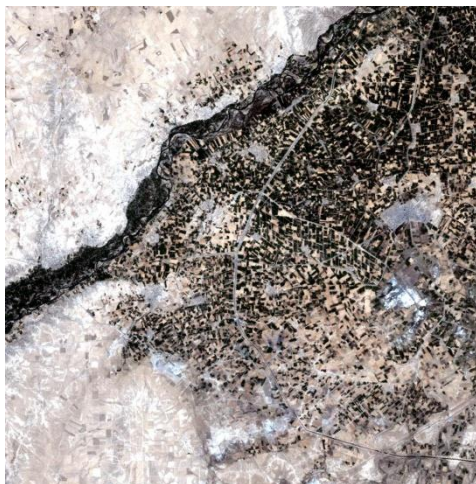


Figure 5- unaffected color version of ETM+ bands acquired in January 23rd 2003.

3.1 Arithmetic Mean Filter

It is non-adaptive filter (also called *box filter*). Let S_{xy} represent the set of coordinates in a rectangular subimage window of size $m \times n$, centered at point (x, y) . The arithmetic mean thus represents the average value within a window of the image $g(x, y)$; i.e. [4]

$$\hat{f} = \frac{1}{mn} \sum_{(s,t) \in S_{xy}} g(s,t) \quad (1)$$

The mean filter has been applied on various multifunction bands of the ETM+ sensor image; i.e. wherever zero values are found they are replaced by the average candidate, using masks of size 3×3 pixels. Figure 6 shows the restored bands by this filter.

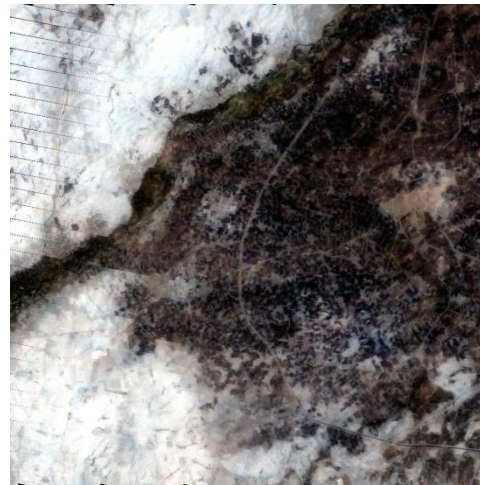


Figure 6- Partially filled ETM+ color scene, using 3×3 mean filter, acquired in May 14th 2010

Obviously, the missing (zero) locations are partially filled. The unfilled locations are because the center pixel within the 3×3 size filter was surrounded by totally malfunction pixels. To overcome this problem, the mean filter operation has been repeated to fill the rest unfilled pixels; the result is shown in Figure 7. Larger size of mean filters could be used to avoid the iteration process but the result will be corrupted by blurring effect.

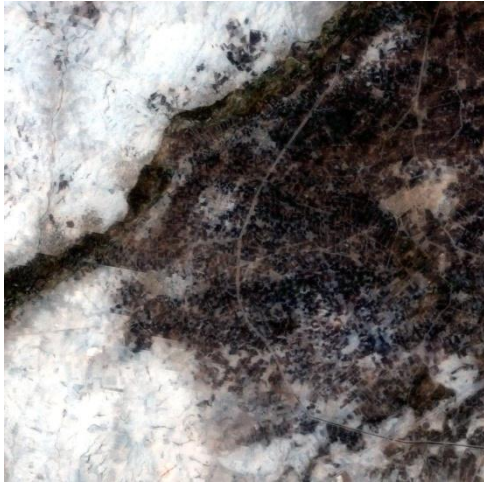


Figure 7- Fully filled ETM+ scene by iterating the 3×3 mean filter twice.

3.2 Median Filtering

The best known order-statistics filter is the median filter, which, as its name implies, replaces the value of a pixel by the median of the gray levels in the neighborhood of that pixel; i.e. [4]

$$\hat{f} = \underset{(s,t) \in S_{xy}}{\text{Median}}\{g(s,t)\} \quad (2)$$

The median filter is normally used to reduce noise in an image; it often does a better job than the mean filter in preserving useful details of high frequency in the image. As it has been done with the mean filter, the median filter of 3×3 size is implemented iteratively two times to restore the malfunction scene; the result is illustrated in Figure 8.

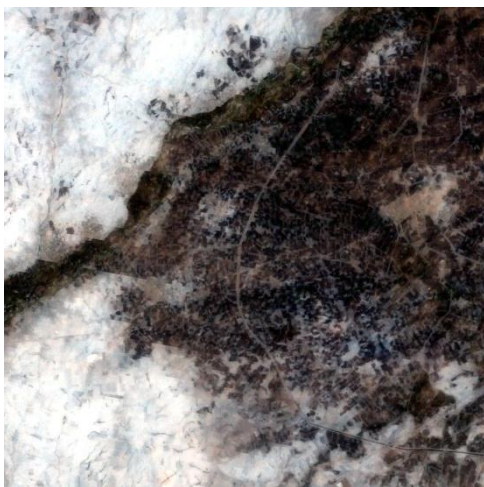


Figure 8- Filled gaps color scene using 3×3 size median filter, iterated twice.

3.3 Midpoint Filtering

The midpoint filter simply computes the midpoint between the maximum and minimum values in the area encompassed by the filter;

$$\text{i.e. [4]} \quad \hat{f} = \frac{1}{2} [\underset{(s,t) \in S_{xy}}{\text{Max}}\{g(s,t)\} + \underset{(s,t) \in S_{xy}}{\text{Min}}\{g(s,t)\}]$$

(3)

Once again, as it has been done with the mean and the median filters, the midpoint filter of 3×3 size is implemented iteratively two times to restore the malfunction scene; the result is illustrated in Figure 9.

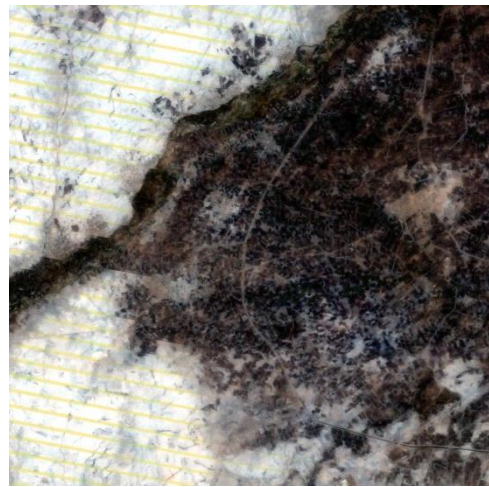


Figure 9- Filled gaps color scene using 3×3 size midpoint filter, iterated twice

As it is obvious, inspecting the scene carefully show color lines replacing the gaps which means that; the replacement of the gap location by the midpoint is not a satisfactory option.

3.4 Simple Replacement Method

In this interpolation method, the locations of malfunction-gaps in the image band to be restored are firstly identified; their corresponding pixel's values in the same band of the other (differently dated acquired image) are defined. The gap filling is then performed by replacing all gaps locations by the corresponding defined pixel's values of the second image. Figure 10 illustrates the replacement results obtained by filling gaps in image bands acquired in May 14th, 2010 by the corresponding pixel's values of the image bands acquired in June 16th, 2010.

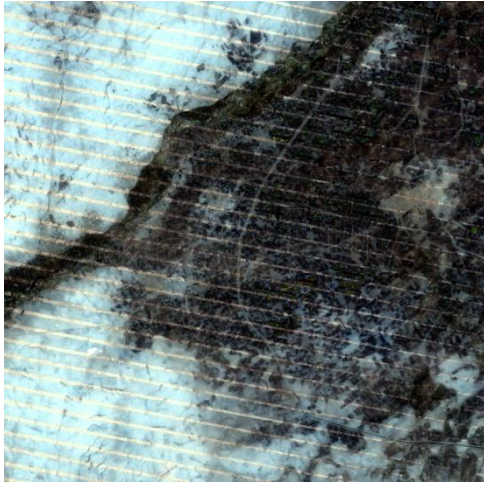


Figure 10- The gap-filled color scene image acquired in May 14th, 2010 by simply replacing its gaps by the corresponding values of the image bands acquired in June 16th, 2010

The imperfection of the simply replacement method is because the gap filled and donor image bands are radiometrically differ; i.e. acquired in different atmospheric seasonal effects (e.g. Sun elevation angle and the Earth-sun distance at the time the images were acquired).

3.5 Interpolating Data

Interpolation is a process for estimating values that lie between known data points. It is important for applications such as signal and image processing and data visualization. The Image Processing tool provides three interpolation methods: *nearest-neighbor interpolation, bilinear interpolation, and bicubic interpolation*

3.5.1 Nearest Neighbor Interpolation Method

For nearest-neighbor interpolation, the output pixel is assigned the value of the pixel that the point falls within. No other pixels are considered. It, thus, the simplest scheme for gray-level interpolation (also called zero-order interpolation), for detail see [4]. In this work, the nearest neighbor interpolation is implemented in one-dimensional form; the non-zero values surrounding the gap (i.e. the zero pixel value) will be inserted in a vector of length "n" equal to the number of the surrounded non-zero values. The gap position is then replaced by nearest neighbor estimation of vector element lies in round $((n+1)/2)$ position. [5]. To be sure that the used window occupying certain number of

surrounding non-zero values, we have adopted window's size 11X11 in performing the interpolation. Figure 11 illustrates the gap filling result obtained by the 1D-nearest neighbor method.

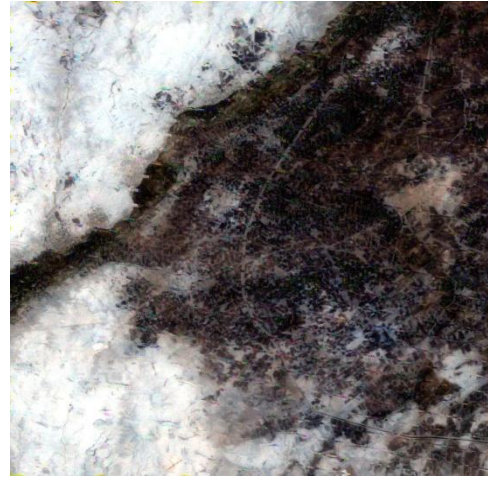


Figure 11- gap filling result obtained by performing 1D-nearest neighbor interpolation method, window's size 11X11 pixels.

3.5.2 Bilinear Interpolation Method

The bilinear interpolation is an extension of linear interpolation. The key idea is to perform linear interpolation first in one direction, and then again in the other direction. Although each step is linear in the sampled values and in the position, the interpolation as a whole is not linear but rather quadratic in the sample location. However, the linear interpolation uses more memory than the nearest neighbor method, and requires slightly more execution time, its results are continuous, but the slope changes at the vertex points, [5]. In our gap filling process, the same operations which have been followed with nearest neighbor interpolation method is carried here, again a window's size 11X11 pixels has also been adopted. Figure 12 illustrates the gap filling result obtained by the 1D-linear interpolation method.

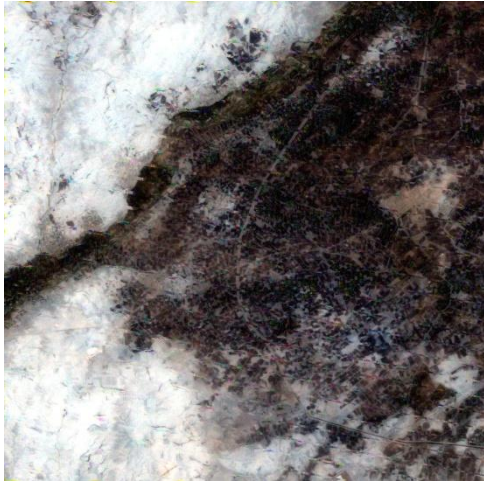


Figure 12- gap filling result obtained by performing 1D-linear interpolation method, window's size 11X11pixels.

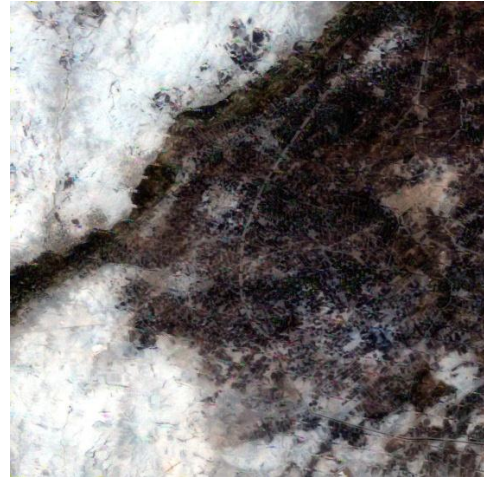


Figure 13-gap filling result obtained by performing 1D-cubic-spline interpolation method, window's size 11X11pixels

3.5.3 Bicubic Convolution Interpolation

In mathematics, *bicubic interpolation* is an extension of *cubic interpolation* for interpolating data points on a two dimensional regular grid. The interpolated surface is smoother than corresponding surfaces obtained by *bilinear interpolation* or *nearest-neighbor interpolation*. *Bicubic interpolation* can be accomplished using *Lagrange polynomials*, *cubic splines*. In image_processing, bicubic interpolation is often chosen over bilinear interpolation or nearest neighbor in image resampling, when speed is not an issue. This method fits a different cubic function between each pair of existing data points, and uses the *spline* function to perform cubic spline interpolation at the data points. It produces the smoothest results of all the interpolation methods. Unexpected results may be obtained by the spline method if the input data is non-uniform and some points are much closer together than others. The procedures followed with the spline interpolation are similar to those performed with nearest and linear interpolation methods, a window of size 11X11 pixels to extract the non-zero values surrounding the gap position, arranging them in a vector form, implementing the spline interpolation to estimate the gap location value. The gap filling result is illustrated in Figure 13.

4. Linear Local Histogram Matching (LLHM)

Variations in solar illumination conditions due to; atmospheric scattering, atmospheric absorption, and detector performance causes differences in radiance values produce dissimilarities to the reflectance of land cover. Absolute radiometric quantification is an expensive, time consuming and likely untenable goal for land-cover and land-use monitoring [6]. Therefore, the primary goal of most change detection studies is to achieve image to-image normalization, so that spatial-temporal differences in image brightness convey information about changes in land cover and land use [7]. Generally, there are two common ways used to radiometric normalization techniques; i.e. dark object subtraction method, [8], and relative radiometric normalization using pseudo-invariant features, [9].

The first step in our gap filling process requires to identify the gap (i.e. zero) and the valid (non zero) pixel's positions in an image to be restored. Once the valid pixels in both the temporal scenes (the image to be restored and the donator image) are located, the linear histogram matching methodology can be attempted to find a linear transformation between them, as shown in Figure 13. The valid pixel values of the donator image can be corrected before transferring them to fill the gap locations of the SLC-off image, the image to be restore, using the gain and bias illustrated in Figure 14, using;

$$Y(x,y) \approx Gain X(x,y) + Bias \quad (4)$$

Where: $Gain = \frac{\sigma_Y}{\sigma_X}$, $Bias = \bar{Y} - Gain \bar{X}$,

and $\bar{Y}, \sigma_Y, \bar{X}, \sigma_X$ are the means and standard deviations of the donator and the SLC-off images, respectively.

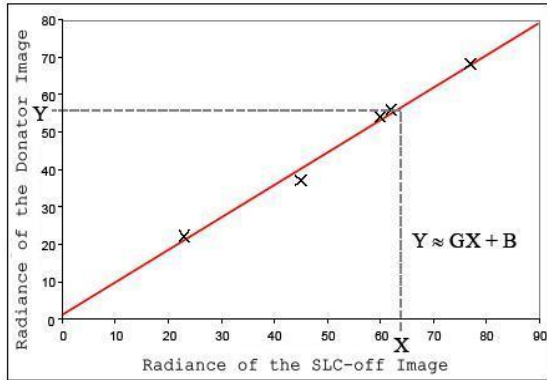


Figure 14- Linear Relationship between the Donator and the SLC-off image radiances.

The LLHM gap filling technique is performed by two ways; i.e.

- The means and standard deviations of the SLC-off and Donator images have been computed for the whole valid pixel values in both images, the result is shown in Figure15.

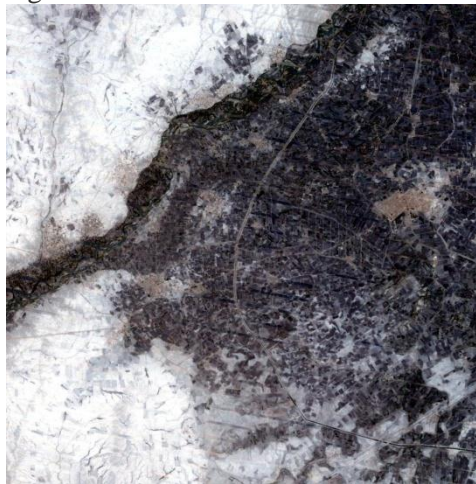


Figure 15- Gap filling result by implementing the LLHM on the whole valid image pixels.

As can be seen, the gaps have been filled with inadequate values. Probably, because the scenes

covers large areas, the radiance effects did not distributed homogenously, and as a consequence the counted Gain and Bias values cannot satisfy the gap filling restoration goal.

- The LLHM filling is performed on segmented images into windows (i.e. the mean and standard deviation values have been computed for each window and individually used to restore the SLC-off image). The result is illustrated in Figure16.

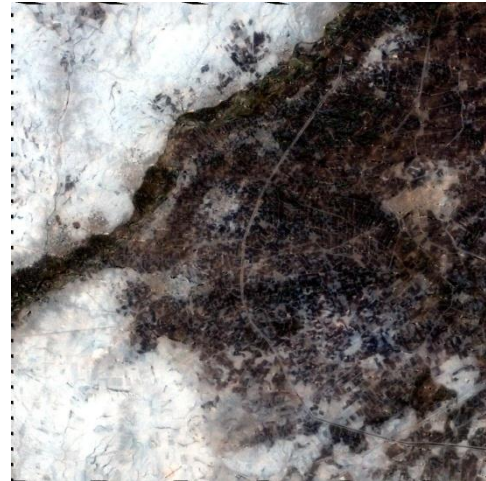


Figure 16- Gap filling result by implementing the LLHM on partitioning images into widows of 11X11 pixels size.

As it is obvious, a better restored image is obtained, except at the image margins some pixels have not filled because the large size window has skipped them. It should be indicated that a large window's size has been adopted to ensure they occupy valid pixel values required to measure the mean and standard deviation values.

5. Quantitative Test

When the level of information loss can be expressed as a function of the original or input image and output processed images, it is said to be based on an *objective fidelity criterion*. A good example is the *peak-signal-to-noise ratio* "PSNR", defined by [10];

$$PSNR = 10 \log_{10} \frac{(L-1)^2}{\frac{1}{NM} \sum_{x=0}^{N-1} \sum_{y=0}^{M-1} [g(x,y) - f(x,y)]^2}$$

(5)

Where: $f(x, y)$ & $g(x, y)$ represent the original image arrays of the input and output images respectively, each of size $N \times M$ pixels, and L is the number of gray levels (e.g. for 8 bits, $L=256$).

The original image “ $f(x, y)$ ” is assumed as that presented in Figure 5 (i.e. unaffected color version of ETM+ bands acquired in January 23rd 2003), while the processed “ $g(x, y)$ ” is regarded as to be the gaps filled obtained by implementing the above mentioned techniques. The resulted PSNR measure, shown in Table1, represents the average value of the PSNR implementing on the RGB bands of the colored image version; i.e.

$$PSNR = \frac{1}{3} [PSNR_{Band1} + PSNR_{Band2} + PSNR_{Band3}]$$

(6)

6. Conclusions

Several gap-filling methods have been tried to restore the ETM+ impacted by the failure of the system’s Scan Line Corrector. The trained methods can be categorized into two types; the first type (i.e. Arithmetic-Mean, Median, Mid-Point, 1D-Nearest-Neighbor, 1D-Linear, and 1D-Spline) do not require an extra temporal scene to fill the gaps, therefore they can be referred to as self-scene-dependent methods. The second type estimating the gap values using a temporally different viewed scene, thus they could be referred as different-scene-dependent methods. Subjectively, the filling results by some of them were good, while others suffered from gap’s missing locations. The missed locations by the Mean, Median, and the Mid-point filters have been manipulated by repeating the filters more than one time, or by increasing the window’s filter size. However, small size filter repetition is preferable to avoid blurring effect. The objective test which has been carried by the PSNR test does not reflect the actual efficiency of the filling method; because the used reference image was acquired in far time of the processed images; i.e. carefully inspecting the gaps-filled images can show the mismatching

Table 1- PSNR measures for the various adopted Gap-filling types

Gap-Filling Method	PSNR Band1	PSNR Band2	PSNR Band3	PSNR Average
Arithmetic Mean 1-Iteration	9.809	9.298	10.384	9.830
Arithmetic Mean 2-Iterations	9.828	9.330	10.450	9.869
Median Filter 2-Iterations	9.826	9.325	10.441	9.864
Mid-point Filter 2-Iterations	9.836	9.329	10.252	9.806
Simple Replacement Method	10.141	9.528	10.579	10.083
1D-Nearest Neighbor Interpolation Method,	9.839	9.353	8.521	9.238
1D-Linear Interpolation Method	9.839	9.353	10.454	9.882
1D-Spline Interpolation Method	9.839	9.353	10.461	9.884
LLHM Image Normalization Method	11.881	10.549	11.430	11.287
LLHM Window Normalization Method	9.789	9.282	10.375	9.815

between the subjective and objective tests. It is our opinion, despite the inefficient PSNR results showed by the LLHM window’s method, it yield a better satisfactory gap’s values replacement than other methods. A few extra procedures may be required to overcome the margining skipping effects obtained by it. Finally, it should be noted that; possibly if a quite matched reference image is available, the fidelity tests (i.e. objective and subjective) will be harmonized.

Reference

1. Jensen, J.R., **2000**, Remote Sensing of the Environment: an Earth Resource Perspective, Prentice Hall, Saddle River, NJ, 544 pp.
2. Bolorani, A.D., Erasmi, S. & Kappas M., **2008**, *Multi-Source Remotely Sensed Data Combination: Projection Transformation Gap-Fill Procedure*, Sensors, **8**, 4429-4440.
3. Lillesand, T. M., Kiefer R. W. and Chipman J. W. **2007**, Remote Sensing and Image Interpretation, 6th Ed., John Wiley & Sons, Inc.
4. Gonzalez, R. C. & Woods, R. E., **2002**, *Digital Image Processing*, 2nd Edition, Prentice-Hall, Inc, New Jersey.
5. De Boor, C., **1978**, A Practical Guide to Splines, Springer-Verlag.
6. Song, C., Woodcock, C.E., Seto, K., Lenney, M.P., Macomber, S., **2001**, Classification and change detection using Landsat TM data: when and how to correct atmospheric effects, Remote Sensing of Environment **75**, 230–244.
7. Roberts, D.A., Batista, G.T., Pereira, J., Waller, E.K., Nelson, B.W., **1998**, Change identification using multi-temporal spectral mixture analysis: applications in Eastern Amazonia In: Lunetta, R.S., Elvidge, C.D. (Eds.), Remote Sensing Change Detection: Environmental Monitoring Methods and Applications, Ann Arbor Press, Chelsea, MI, p. 318.
8. Chavez, P.S., **1996**, Image-based atmospheric corrections revisited and improved, Photogrammetric Engineering and Remote Sensing **62**, 1025–1036.
9. Schott, J., Salvaggio, C., Volchok, W., **1988**, Radiometric scene normalization using pseudo-invariant features, Remote Sensing of Environment **26**, 1–16.
10. Umbaugh Scott E, **1998**, Computer Vision and Image Processing, Prentice Hall PTR, Inc., A Simon and Schuster Company, Upper Saddle River, NJ 07458.